Soil & Environmental Health 1 (2023) 100046

Contents lists available at ScienceDirect

Soil & Environmental Health

journal homepage: www.sciencedirect.com/journal/soil-and-environmental-health

Research Paper

Estimating soil health in urban allotments: Integrated two-way soil quality index and free-living amoebae in nitrogen recycling

Roderick A.M. Williams [a,*], Andrea Ogoke [a], Kiri Rodgers [a], Steven Kelly [a], Roslyn Mcintosh [b,c], Andrew Hursthouse [c], Fiona L. Henriquez [a]

[a] Institute of Biomedical and Environmental Health Research, School of Health and Life Sciences, University of the West of Scotland, Lanarkshire Campus, Stephenson Place, Blantyre, G72 0LH, UK
[b] Inverclyde Council, Municipal Buildings, Clyde Square, Greenock, PA15 1LY, UK
[c] School of Computing, Engineering & Physical Sciences, University of the West of Scotland, Paisley PA1 2BE, UK

HIGHLIGHTS

- A hybrid soil quality index was developed to assess soil health.
- Index incorporated soil chemical and biological properties.
- Aluminium contamination impacted soil health, ecosystem services, and microorganisms.
- *Acanthamoeba* was important in N-recycling to maintain soil health.
- *Acanthamoeba* converts nitrates to ammonium via nitrate reduction enzymes.

GRAPHICAL ABSTRACT

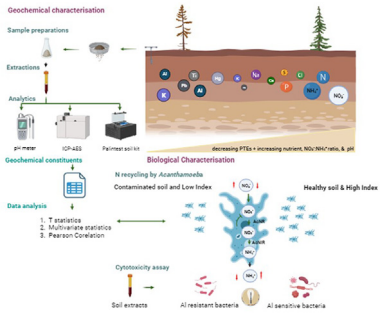

ARTICLE INFO

Handling Editor: Lena Q. Ma
Technical Editor: Lena Q. Ma

Keywords:
Soil health
Potentially toxic elements
Amoeba *Acanthamoeba*
Nitrogen recycling
Soil quality index
Urban allotments
Biological biomass
Geochemical constituent

ABSTRACT

Nitrogen deficiency and contamination by potentially toxic elements (PTEs) adversely impact soil health and ecosystem services. Existing tools for assessing contaminated soils, necessary for sustainable management, remain limited. In this study, we introduce an integrated approach using geochemical constituents and biological factors to construct a comprehensive index to evaluate contaminant impacts on soil health. We collected samples in triplicate from six plots within an urban allotment with a history of PTE contamination. Selected biological and chemical characteristics of the samples were quantified to derive impact scores, with a single numerical index representing overall soil quality for each plot. Multivariate, T-statistics and Pearson Correlation analysis were used to identify relationships and differences between selected soil parameters between plots. The role of the free-living amoeba *Acanthamoeba* in nitrogen recycling was assessed with feeding experiments, enzymatic assays and bioinformatics analysis. The plot with the highest index value, indicative of good health, exhibited higher pH, significantly high microbial load, and a high nitrate to ammonium (NO_3^-:NH_4^+) ratio of 5.3. This turnover was associated with *Acanthamoeba* uptake of exogenous nitrates and secretion of ammonium, through the assimilatory/dissimilatory nitrate reduction pathway. In contrast, the lower index plot with the low nitrogen turnover of 0.69, showed elevated aluminium, low pH activity and a significantly reduced microbial load, dominated by

* Corresponding author.
E-mail address: Roderick.williams@uws.ac.uk (R.A.M. Williams).

https://doi.org/10.1016/j.seh.2023.100046
Received 16 October 2023; Accepted 16 October 2023
Available online 19 October 2023

aluminium resistant microorganisms. Our findings highlight the importance of a comprehensive soil quality index by integrating multiple characteristics to assess soil health and contamination. The approach addresses the need for improved tools to identify the direct impact of contaminants on soil biological activity, supporting more sustainable land management.

1. Introduction

Soils encompass an intricate and ever-changing ecosystem, interweaving chemical components and microbial biomass that collectively define soil health. These interactions drive vital processes such as nutrient cycling, organic matter decomposition, the regulation of proton activity, soil structure formation, and resilience (Bastida et al., 2021). Thus, soil health is of paramount importance for sustainable land management, and enhancing agricultural productivity and high level of environmental protection. The conservation of natural resources requires good understanding of approaches to comprehensive evaluation (Lehmann et al., 2020).

Existing soil quality indices, including the Soil Management Assessment Framework (Ylagan et al., 2021), Cornell Soil Health test (Idowu et al., 2009) and variations developed in different geographical regions, e.g., New Zealand (Lilburne et al., 2004), Australia, (Gonzalez-Quinones et al., 2011), Europe (Huber et al., 2001) and China (Teng et al., 2014) to gauge soil health, rely predominantly on physicochemical data collected on basic chemical components, which may have an inherent bias. They emphasise static evaluations from total instead of the extractable forms of the analytes that encapsulate dynamic nature of soil health (Mukherjee and Lal, 2014; O'Neill et al., 2005). The biological dimension that recognises the living nature of soil is generally overlooked, rendering these indices less effective for formulating adaptable land management strategies (Balaram, 2021). There are however biological indices, based on activities such as soil respiration and biomass of certain organisms, e.g., bacteria, nematodes, arthropods, or earthworms (Trivedi et al., 2017; Moran et al., 1996), which provide opportunities for the assessment of wider soil ecosystem function, but these are seldom included in the suitability evaluation of soil for change of end use. We postulate that integrating the biological and biochemical parameters into a single index will provide a holistic understanding of soil health, which is robust enough to inform the development of effective management strategies (Mukherjee and Lal, 2014).

In recognition of this need, this study focuses on using the free-living soil amoebae *Acanthamoeba* as a surrogate for eukaryote diversity. We propose that *Acanthamoeba*'s sensitivity to environmental changes (Khan, 2006), its role in nutrient release, recycling, bacterial abundance regulation (Sinclair et al., 1981) and its association with human diseases (Khan, 2006), make it a suitable model organism for unravelling the complexity of soil health determination.

A threat to soil health stems from potentially toxic elements (PTEs), which are chemical elements that, at certain concentrations, can pose risks to human health and the environment due to their toxic properties. This threat is particularly pronounced in urban areas where PTEs can exceed regulatory limits, compromising functional land use and utilisation. Urban spaces, including allotment gardens (public greenspace created for personal food production), often contain elevated PTEs from past industrial activities and traditional historic gardening practice, necessitating vigilant monitoring and remediation for sustainable land management. In Scotland, 82% of urban spaces contaminated with Pb, Zn, As, Cu, and/or Cd (Alloway and Ayres, 1993) are designated as vacant and derelict land (Scotland. Communities Analytical Services), with 75% of them being allotments (Scotland. Communities Analytical Services). These elements exhibit toxicity at specific levels, which can pose hazards to both ecosystems and human well-being through intricate channels such as the food chain (Liu et al., 2020). Despites remediation efforts, progress in revitalising Scotland's derelict lands remains gradual with only 6% reduction reported in certain contaminants between 2017 and 2018 (Scotland. Communities Analytical Services). Major challenges for the remediation of urban topsoil are dealing with the recontamination risks through potential exposure pathways for human health and protection of surface and groundwater through leaching.

To purse the development of a dynamic index capable of effectively monitoring and addressing these challenges, we conducted a study within an urban allotment previously identified by local authority assessment and recognised for its diverse physicochemical properties, cultivated plants, and varied gardening practices of plot owners over many decades of use (Bechet et al., 2018). The controlled environment of the allotment garden serves as a pivotal platform for the long-term monitoring of soil health changes and vulnerability to recontamination. Notably, urban allotments are consistently enriched with fertilisers containing elements such as Mg, K, N and P, capable of altering soil pH, nutrient bioavailability and biomass content, subsequently amplifying soil biological output (Schoenholtz et al., 2000). The multiple oxidation states of N control their impact on soil fertility and make them available for various metabolic pathways within soil ecosystems (Wu et al., 2005; Pintro et al., 1996). Moreover, the regulation of soil by N-fixing bacteria has also emerged as a key determinant of soil health. For example, nitrate (NO_3^-) uptake by bacteria and its conversion to nitrites (NO_2^-), and ammonium (NH_4^+) via the assimilatory nitrate reduction pathway, orchestrated by enzymatic activities of nitrate and nitrite reductases, play a significant role (Nelson et al., 2016). The NH_4^+ dispersed into the external milieu, influence soil microbial diversity and abundance, emphasizing the significance of the NO_3^-:NH_4^+ ratio (Maeda et al., 2011). The reciprocal ammonification pathway, replenishes soil nitrates, further highlighting the role for N-fixing bacteria in governing soil vitality (Yao et al., 2013; Maeda et al., 2011; Einsle et al. 1999, 2000; Bargaz et al., 2018; Wu et al., 2005). This emphasises the opportunity to integrate a biological component into existing soil health indices.

In summary, the ubiquitous risk posed by PTEs challenges soil health, especially in urban areas, necessitating vigilant monitoring and often a need for active remediation. This study uses an urban allotment garden with diverse characteristics to facilitate the development of a dynamic index capable of capturing these complexities. This approach, anchored in both physicochemical and biological parameters, supplemented by the biomass of *Acanthamoeba* as a eukaryotic surrogate, demonstrates opportunities to be gained from a deeper comprehension of soil health and contamination. It aligns with the One Health framework that intertwines soil health, ecosystem dynamics, and human well-being, to foster a holistic approach to soil health evaluation. The findings of this study provide an opportunity to define and establish more sustainable land management strategies.

2. Methodology

2.1. Soil sampling

The procedures used in this study followed the guidelines of the University of the West of Scotland Ethics Committee and was approved by this Committee (approval number 17-5-16- 001).

An allotment located in the West of Scotland characterised by a diverse range of environmental pressures and land use patterns were chosen as the study site (Fig. 1 (Bechet et al., 2018)). Soil samples were

Fig. 1. Schematic representation of plots in the Wellington allotment. The map of Scotland with the study area marked in blue. The region is enlarged to showcase the allotment and plots represented as black boxes. The six plots surveyed are numbered. Light grey boxes represent residential houses along the road bordering the allotment. Trees are represented with green stars.

collected from 6 out of 30 allotment plots, encompassing the varied land use patterns (Bechet et al., 2018). The plots were designated MP1, MP2, MP3, MP5, MP6 and MP12. The sampling procedure involved using a coring device to obtain samples to a depth of 20 cm. Triplicate samples were collected from three randomly chosen spot, within each plot to account for spatial variability. Soil samples designated for biological analysis were stored at 4 °C while samples for physicochemical analysis, were pooled, dried at 40 °C until a constant weight was achieved and sieved to <2 mm particle size. The samples were stored at room temperature.

2.2. Extraction and analytical protocols of geochemical constituents and minor soil nutrients

Two extraction and analytical procedures were used to assess the geochemical constituents and minor soil nutrients. For evaluating extractable contents, the Palintest soil test kit (SKW500, Palintest, Gateshead, NE11 0NS, UK) was utilised. The pH was measured using a soil suspension prepared by mixing 2 g of dried soil mixed with 10 mL of deionised water using a Multiparameter Pocket Sensor. Lime requirement estimation (g/m^2) involved adding one liming buffer tablet to the soil suspension prepared as described above. The resultant modified proton activity obtained from the Multiparameter Pocket Sensor set as the pH measurement mode was converted to lime requirement using the lime requirement table for organic soils provided by the manufacturers. Soil electrical conductivity (EC) was estimated as µS/cm or mS/cm using soil suspension prepared from with 1 g of soil in 10 mL of deionised water and the conductivity mode on the multiparameter pocket sensor was utilised for this measurement. Total Organic matter (OM) content was determined using loss-on-ignition. Briefly, 5 g of soil was dried at 105 °C overnight and then heated in a muffle furnace at 450 °C for 2 h. The OM was calculated as a percentage based on the weights at of the quotient of the differences between the weights at 105 °C and 450 °C. Additionally, total organic carbon (OC) was estimated by multiplying OM with a conversion of 1.72 (Hoogsteen et al., 2015).

The micro and macro nutrients termed geochemical constituents (GCCs) were extracted using the Palintest soil kit and aqua regia extraction protocols coupled with the Thermo Electron iCAP 6000 series ICP-AES. Additional information can be found in Supporting Information. The recovery rate for each GCC was estimated using known quantities of laboratory stock solutions for each nutrient prepared. These nutrients were subjected to the GCC-specific extraction protocol described previously. The concentrations of the GCCs were determined at different levels covering a wide range of concentrations within the linear range of the analytical instruments used for total and extractable nutrients analysis. The recovery rate for each GCC was calculated using the formula:

Recovery rate (%) = [(Measured concentration of nutrient after extraction) / (Known concentration of nutrient before extraction)] x 100

The recovery rates for each nutrient were determined on triplicate samples.

2.3. Cell culture and cell density estimations

Soil suspensions containing bacteria were obtained by the method in (Ben-David and Davidson, 2014). One-gram (1 g) of soil was mixed with 1 mL of double distilled water, left to settle and 100 µl of the settled suspension streaked out in Luria Bertani (LB) agar which was incubated for up to 72h at 25 °C, 37 °C and 55 °C to capture the wide range of microbial diversity. After incubation, colonies grown on the solid medium was counted and the results expressed as colony forming units per gram of soil (CFU/g). Al-resistant bacteria were culture in LB agar impregnated with 10 mM Al and incubated at 37 °C. Individual colonies were selected and cultured in LB broth with or without Al and at temperatures corresponding to initial culture temperatures and pH defined by the experimental protocol.

Lab-derived *Acanthamoeba castellanii* (ATCC50370) were grown in liquid Peptone-Glucose (PG) medium at 25 °C until reaching confluence (up to 5 days). For Al cytotoxicity assay, *A. castellanii* (10^5) were culture in PG at pH 3.6, pH 4.6 and pH 8.6 with 10 mM Al serially diluted 11 times and incubated at 25 °C for 96 h. Viability was estimated with the Alamar blue assay at absorbances of 597 nm and 600 nm (McBride et al., 2005) and the dose that kills 50% of cells (IC_{50}) was estimated with the Grafit software. Soil-derived *Acanthamoeba* species in soil suspension were isolated from a mixture of 1 g of soil in 1 mL of double distilled water. The suspensions (100 µL) were placed onto non-nutrient agar plates containing 1% (v/v) penicillin-streptomycin and incubated for up to 6 weeks to allow the development of *Acanthamoeba* cysts colonies which were monitored daily using microscopy. *Acanthamoeba* cysts were transferred to liquid PG medium, and cell density was estimated using a haemocytometer. Viability of *Acanthamoeba* was assessed using the Alamar blue assay (McBride et al., 2005).

2.4. Estimation of NO_3^- and NH_4^+ levels in media and Acanthamoeba species

The concentrations of NO_3^- and NH_4^+ were determined using pellets of confluent lab-derived *A. castellanii* at a concentration of 1×10^4 cells/mL. The corresponding extracellular soils (designated as spent medium) were also analysed. These measurements were conducted using three methods (a) the Palintest soil kit, NO_3^- and NH_4^+ options described previously, (b) the Griess reagent within the nitrite/nitrate assay kit (Sigma Aldrich, UK), and (c) Ammonium assay kit (Sigma Aldrich, UK). PG medium with no cells was used as a control. All experiments were carried out following the instructions provided by the manufacturers. Absorbance values of nitrate and nitrite were converted to micromoles using a standard curve. Percentage NO_3^- and NH_4^+ uptake and/or release were calculated by comparing intracellular data with control experiments for cells and spent media. Protein concentrations used for normalization was estimated using Bradford assays (BioRad, UK). All experiments were carried out in triplicate.

2.5. DNA extraction

Total soil DNA was extracted using the Zymo Research Soil Microbe DNA MiniPrep kit (Catalog No. D6001) following the manufacturer's instruction. For bacteria cells were harvested from cultures by centrifugation at 3000×*g* for 10 min. Genomic DNA was then extracted by lysing the bacteria using 10% SDS solutions (w/v). For *A. castellanii*, the same harvesting method was used, and lysis was achieved using a modified UNSET buffer containing Urea (8 M), Sodium Chloride (NaCl, 50 mM), SDS (1%), ethylenediaminetetraacetic acid (EDTA, 10 mM), Tris-HCl (50 mM), pH7.5 (100 µL) (Ertabaklar et al., 2007). After cell lysis, equal volumes of phenol:chloroform (1:1; 200 µL) added to the lysate. The precipitated DNA was washed with 100% ethanol (v/v), repeated three time by centrifugation at 13,000×*g* for 15 min. The DNA pellets were air dried and resuspended in double distilled water. The concentration of the extracted genomic DNA (gDNA) was quantified using the Nanodrop® Spectrophotometer (Thermo Scientific, NanoDrop®-1000).

2.6. PCR amplification of biological markers in soil microbes

The DF3 region of the 18s rRNA of *Acanthamoeba* was amplified from total soil DNA using the GoTaq system (Promega). The Polymerase Chain Reaction (PCR) reaction was performed in 50 µL with gene specific forward and reverse primers named JDF1 (5'-GGCCCAGATCGTTTACCGTGAA-3') and JDF2 (5'-TCTCACAAGCTGCTAGGGGA-GTCA-3'). For amplification of the 16s rRNA of prokaryotes, the primers 27f (5'-AGAGTTTGATCATGGCTCAG-3') and the 1429r (5'-TACGGYTACCTTGTTAGCACTT-3') were used. The PCR mix for both were prepared according to manufacturer guidelines. They consisted of 10 µL of 1X GoTaq flexi buffer, 4 µL 1.0–4.0 mM $MgCl_2$, 5 µL dimethyl sulfoxide (DMSO), 1 µL 0.2 mM deoxyribonucleoside triphosphates (dNTPs), 0.5 µL 1.25 U GoTaq DNA Polymerase, 0.5 µg gDNA samples and 5 µL of JDF1 and JDF2 primers. The PCR cycle was and initial 95 °C for 2 min followed by 35 cycles of denaturation at 95 °C for 1 min, annealing at 60 °C for 1 min and extension at 72 °C for 1 min. A final elongation step was performed at 72 °C for 5 min. The amplified products were resolved by agarose gel electrophoresis cloned into the T-vector and sequenced by Eurofins MWG using the universal primers, T7 and SP6.

2.7. Using qPCR to estimate Acanthamoeba numbers in soil

DNA extracted from soils diluted with Tris-EDTA (TE) buffer (1 M Tris-HCl, pH8.0 and 0.5 M EDTA) was used in qPCR reactions conducted on a StepOnePlus real time PCR system (Applied Bioscience). The 180-bp DNA segment on *Acanthamoeba* 18S rDNA quantification was achieved using the SYBR Green qPCR system (Sigma Aldrich). Each reaction mix (25 µL) contained 10 µL SYBR Green, 0.25 µL forward primer, JDF1, 0.25 µL reverse primer, JDF2, 1 µL DNA, and PCR grade sterile water (Roche Diagnostics). The thermal program for amplification was set at an initial denaturation step at 95 °C for 10 min, followed by 50 cycles at 95 °C for 15 s, annealing at 60 °C for 1 min, extension at 72 °C for 1 min and a final cooling at 72 °C for 5 s. Each qPCR run consisted of test samples, serially diluted DNA standards prepared from known cell densities of *A. castellanii* and no template control. The anti-log cycle threshold (Ct) value of the DF3 region of the 18srRNA in total genomic DNA of *Acanthamoeba*, amplified by RT-PCR using the JDF1 and JDF2 produce a standard curve with the linear equation y = 2E+09x - 6E+07, R^2 = 0.9981. To determine the DNA concentration in the test samples, Ct values corresponding to log *Acanthamoeba castellani* cell density/mL) was used.

2.8. Molecular identification and classification of genes and gene products in soil microbe gene content

Bacteria and *Acanthamoeba* species identification were carried out using the translated amino acid sequences of the 16srRNA and 18srRNA as query in BLAST analysis against the non-redundant databases, GenBank and Amoeba bioinformatics resource (www.amoebadb.org). Genes of the dissimilatory reduction pathway in *A. castellanii* gene content were identified with the same method using orthologues from other taxa as query as described in (Williams et al., 2012). A cut-off Expectation value (E-value) of 10^5 from each BLAST searches and sequence alignments, and the presence of peculiar motifs consistent with function were used to validate an identity. For comparative analysis, sequence alignments and phylogenetic trees of the 16srRNA DNA, 18srRNA DNA fragments from bacteria and *Acanthamoeba* spp. respectively as well as the translated amino acid sequences of genes of the dissimilatory nitrate reduction pathway with orthologues from other taxa obtained from GenBank (Kumar et al., 2008) were generated using the Molecular Evolutionary Genetics Analysis software (MEGA).

2.9. Development of the dynamic Soil quality index

To develop the Soil Quality Index (SQI), biological and chemical parameters were selected based on scientific rigor, and ability to evaluate ecological significance and critical aspects of soil health, functionality and sustainability. A selection of parameters, which are known to impact soil health, such as the extractable chemical parameters, proton activity, lime requirement, OM, OC, and extractable nutrients; N, P, K, Mg, Ca, Mn, Fe, Cu, S, and NH_4^+, were selected for the SQI. This was based on their contribution to assessing soil's capacity to retain water, neutralise acidity, promote nutrients recycling and enhance nutrient availability while Al for impact on soil contamination. Total K, Mg, Ca, Mn, Fe, Cu, Zn, Ni, Co, Mo, and Ti were selected for its contribution soil quality, Na on salinity levels, while As, Cd, Cr, Pb and Al as PTEs that indicated contamination risks, commonly enriched above local background levels [31]. For the biological parameters, total bacteria abundance (cfu/mL), *Acanthamoeba* abundance (cells/mL), and total soil DNA (µg/mL) were considered for their role in nutrient cycling, organic matter decomposition, and overall soil biological activity.

The scoring system was developed on a running scale ranging from 0 to 3, indicative of their impact on soil health, ecosystem functionality, and biodiversity. The higher score of 3 represented the maximum positive impact, while progressively lower scores represented reduced impact through to negative impact at 0 (O'Neill et al., 2005; Mukherjee and Lal, 2014).

To prepare the SQI, the abundances of each parameter were used to determine their scores. The scores derived for all parameters in each plot were then summed up to create the unified SQI. Finally, the SQI from each plot was expressed as a percentage of the maximum possible score value estimated to be 54 (based on the 18 parameters used).

2.10. Multivariate statistics

Multivariate statistical analyses were used to assess correlations between the biological and chemical parameters used as soil health indicators, serving to validate the sensitivity and accuracy of the index devised. These test were performed using the MetaboAnalyst Software (https://www.metaboanalyst.ca/(Xia et al., 2009)). Briefly, GCCs and biomass data were prepared in CSV format, in columns and rows, to facilitate data pre-processing and normalization. Specific visualization outputs, including biplots, heatmaps, and principal component analysis (PCA), were generated to identify multivariate patterns in the data using the required functional within the software. T statistics was used to test significance different of each parameter in two plots at the 95% confidence interval.

3. Results

3.1. Extraction protocol for extractable geochemical constituents (GCCs) from soils

3.1.1. Characteristics of the Wellington Allotment soil based on extractable GCCs

The recovery rates for extractable GCCs were generally high, exceeding 90%, with the exception of Mn and Mg, which exhibited lower recovery rates at 59% and 39%, respectively. Analysis of the soil characteristics across six plots showed a predominantly slightly acidic to neutral pH range with pH 5.16 (MP5) to pH 6.94 (MP6), displaying statistical significance across plots ($p < 0.05$; Table 1). EC values were within the low to normal range, spanning from 10.6 (MP3) to 93.2 μS/cm (MP5) indicating non-saline to slightly saline conditions and statistical different across all plots ($p < 0.05$; Table 1)). The OC content ranged from 9.35% (MP1 and MP2) to 13.4% (MP6), while CEC ranged from 10.67 cmol/kg (MP5) to 19.91 cmol/kg (MP6; Table 1). Lime requirement ranged between 400 g/m^2 (MP3 and MP5) to 1500 g/m^2 (MP5; Table 1).

The extractable GCCs, Mg, K, Ca, Mn, Fe, Cu, NO_3^-, P, S, Cl and NH_4^+ showed significant variations across the plots ($p < 0.05$). Ca, remained relatively constant while Al was notably high in MP5 compared to other plots ($p < 0.05$). The estimate for NO_3^-:NH_4^+ratio ranged from of 0.69 in MP5 and 19.34 in MP2 indicated a high turnover in the latter. Heatmaps highlighted elevated levels of Al, P, and Mn in MP5 (Fig. 2A, yellow), while MP6 showed higher levels of Ca, Fe, S, K, Mg, and NH_4^+. (Fig. 2A, magenta).

Pearson correlation coefficients (R^2) between the edaphic factors, pH, OC, EC, OC, and CEC with extractable GCCs showed that proton activity positively corelated with Mg, Ca, S, and CEC ($R^2 = 0.5–0.85$) except for EC, Al, Mn and P ($R^2 = 0.67–0.74$) which displayed negative correlations (Table S1). EC displayed positive correlations with P, lime content, Al and Mn ($R^2 = 0.51–0.97$) while showing negative correlations with CEC and Ca ($R^2 = 0.57–0.68$). OC was positively correlation with K, Fe, S, NH_4^+, CEC, and Mg ($R^2 = 0.50–0.96$), similarly so was CEC with pH, OC, Mg, K, Ca ($R^2 = 0.50–0.97$; Table S1). CEC had a negative correlation with lime content, Al, P, and EC ($R^2 = 0.52–0.78$; Table S1)).

Inter GCCs correlations were observed with Mg positively associated with K, Fe, S and NH_4^+ ($R_2 = 0.51–0.80$) and similarly, K, with Fe, S and NH_4^+ ($R^2 = 0.55–0.81$; Table S1). Al exhibited positive correlation with P

Table 1
GCCs estimated from 6 plots of an allotment using two soil extraction and analytical methods ([a]extraction/analytical).

	Parameters	MP1	MP2	MP3	MP5	MP6	MP12
[a]Palintest extraction/ Palintest spectrometry	pH (mV)	5.89 ± 0.00	6.25 ± 0.13	6.74 ± 0.07	5.16 ± 0.02	6.94 ± 0.04	6.65 ± 0.10
	EC (μS/cm or mS/cm)	33.30 ± 1.01	36.43 ± 0.55	10.63 ± 0.01	93.20 ± 0.23	34.89 ± 0.91	9.47 ± 0.07
	Modified pH (mV)	6.11 ± 0.49	6.37 ± 0.7	6.85 ± 0.10	5.69 ± 0.00	6.76 ± 0.07	6.63 ± 0.07
	Lime g/m2	1000.00 ± 57.73	1000.00 ± 47.73	400.00 ± 28.86	1500 ± 76.38	400 ± 30.23	400 ± 28.67
	OC%	9.35 ± 0.13	9.35 ± 0.15	9.61 ± 0.13	9.41 ± 0.16	13.47 ± 0.77	10.61 ± 0.56
	OM%	16.12 ± 0.09	16.12 ± 0.10	16.56 ± 0.08	16.22 ± 0.13	23.22 ± 0.16	18.30 ± 0.02
	Mg	52.0 ± 1.52	126.0±	117.0 ± 1.96	56.0 ± 1.65	207.0 ± 2.12	80.0 ± 1.64
	K	85.0 ± 1.53	115.0 ± 2.64	114.3 ± 2.31	85.0 ± 1.67	280.0 ± 5.51	140.7 ± 2.45
	Ca	3000.00 ± 205.02	3000.00 ± 221.23	3000.00 ± 196.12	2000.00 ± 150.56	3500.00 ± 169.96	3250.00 ± 217.76
	Al	4.74 ± 0.12	3.03 ± 0.23	0.00 ± 0.00	68.29 ± 0.45	0.14 ± 0.11	1.06 ± 0.12
	Mn	13.70 ± 0.23	5.40 ± 0.12	3.70 ± 0.34	13.50 ± 0.28	6.50 ± 0.34	5.20 ± 0.87
	Fe	33.00 ± 0.66	40.00 ± 0.54	45.00 ± 0.29	57.00 ± 0.54	81.00 ± 0.81	47.00 ± 0.76
	Cu	39.30 ± 0.81	43.90 ± 0.83	52.60 ± 0.27	23.00 ± 0.69	25.10 ± 0.99	21.40 ± 0.23
	NO_3^-	24.70 ± .12	105.00 ± 0.23	51.80 ± 0.34	32.30 ± 0.54	22.10 ± 0.98	20.90 ± 0.28
	P	115.70 ± 2.12	102.00 ± 1.84	70.60 ± 1.34	230.20 ± 1.38	122.10 ± 2.11	51.10 ± 2.16
	S^-	0.00 ± 0.00	0.00 ± 0.00	7.14 ± 0.12	0.00 ± 0.00	14.29 ± 0.14	2.86 ± 0.01
	NH_4^+	7.43 ± 0.16	5.43 ± 0.19	14.64 ± 0.25	6.29 ± 0.29	31.86 ± 0.25	7.64 ± 0.11
	Cl^-	375.00 ± 1.00	375.00 ± 1.12	375.00 ± 0.98	250.00 ± 1.45	250.00 ± 1.28	375.00 ± 1.69
	Na	N/A	N/A	N/A	N/A	N/A	N/A
	CEC cmol/kg	15.64 ± 0.12	16.33 ± 0.23	16.25 ± 0.45	10.67 ± 0.65	19.91 ± 0.45	17.26 ± 0.22
[a]Aqua Regia/ICP-AES	Mg	50.00 ± 0.98	42.00 ± 0.82	48.00 ± 1.10	42.00 ± 1.56	37.00 ± 0.69	7.00 ± 0.79
	K	5.93 ± 0.24	6.57 ± 0.45	7.23 ± 0.23	6.31 ± 0.54	9.16 ± 0.37	7.09 ± 0.76
	Ca	77.47 ± 1.00	114.17 ± 1.10	96.17 ± 1.45	62.65 ± 0.95	109.81 ± 0.99	100.54 ± 1.03
	Al	184.34 ± 1.11	146.64 ± 1.23	182.29 ± 0.67	161.17 ± 0.87	120.75 ± 1.28	128.43 ± 1.34
	Mn	6.05 ± 0.00	5.64 ± 0.62	7.08 ± 0.03	6.31 ± 0.06	5.02 ± 0.08	5.13 ± 0.01
	Fe	238.07 ± 1.56	217.73 ± 1.38	283.60 ± 1.23	243.93 ± 1.33	201.11 ± 1.45	209.73 ± 1.56
	Cu	1.87 ± 0.01	1.37 ± 0.02	1.95 ± 0.03	1.34 ± 0.05	1.10 ± 0.02	1.02 ± 0.02
	Na	4.34 ± 0.11	18.16 ± 0.19	12.91 ± 0.13	19.89 ± 0.45	18.10 ± 0.45	18.22 ± 0.33
	As	0.08 ± 0.00	0.07 ± 0.00	0.12 ± 0.00	0.10 ± 0.00	0.06 ± 0.00	0.07 ± 0.00
	Cd	0.02 ± 0.00	0.02 ± 0.00	0.04 ± 0.00	0.02 ± 0.00	0.01 ± 0.00	0.01 ± 0.00
	Co	3.74 ± 0.12	3.19 ± 0.15	4.34 ± 0.13	3.22 ± 0.21	2.82 ± 0.28	0.01 ± 0.00
	Cr	0.16 ± 0.01	0.15 ± 0.03	0.20 ± 0.04	0.15 ± 0.03	0.14 ± 0.06	2.98 ± 0.10
	Mo	0.02 ± 0.00	0.02 ± 0.00	0.02 ± 0.00	0.02 ± 0.00	0.02 ± 0.00	5.13 ± 0.00
	Ni	0.37 ± 0.01	0.31 ± 0.03	0.42 ± 0.01	0.32 ± 0.04	0.33 ± 0.03	0.018 ± 0.01
	Pb	11.00 ± 0.14	10.00 ± 0.01	14.00 ± 0.12	13.00 ± 0.15	12.00 ± 0.15	15.00 ± 0.16
	Ti	7.00 ± 0.02	66.00 ± 0.42	7.00 ± 0.02	7.00 ± 0.06	4.00 ± 0.06	11.00 ± 0.87
	Zn	6.00 ± 0.10	7.00 ± 0.20	9.00 ± 0.31	6.00 ± 0.21	7.00 ± 0.21	5.00 ± 0.33
	CEC cmol/kg	83.29 ± 0.02	101.23 ± 0.00	95.03 ± 0.01	76.15 ± 0.12	95.57 ± 0.03	65.76 ± 0.03

[a] - CEC = Cation-exchange capacity.

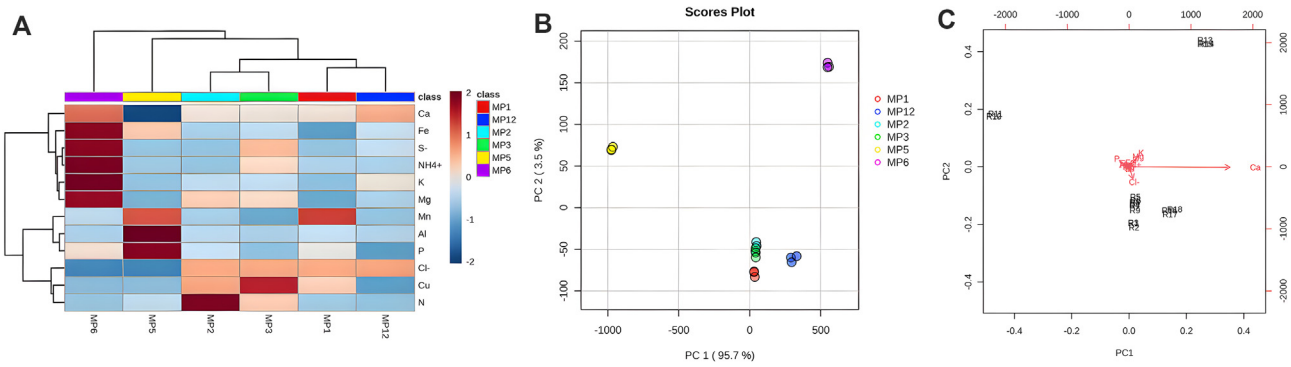

Fig. 2. Multivariate analysis of the GCCs content in 6 plots of an allotment from Palinstest soil extracts. heatmap (A), PCA (B) and (C) biplot analysis of GCCs extracted from 1g of soil suspension using the Palintest soil extraction protocol analysed with the Soiltest 10 photometer. Key for replicates in each plot: MP1, R1-3; MP2, R4-6; MP3, R7-9; MP5, R10-12; MP6, R13-15; MP12, R16-18.

(R^2 = 0.82); Mn with P (R^2 = 0.55) and S and NH_4^+ (R^2 = 0.95; Table S1). Conversely, Ca was negatively correlation with Al (R^2 = 0.86) and P (R^2 = 0.63) while P was with Cl (R^2 = 0.58). Fe displayed mixed correlations being positively associated with S (R^2 = 0.63) and NH_4^+ (R^2 = 0.69) but negatively with Cl (R^2 = 0.71; Table S1).

Principal Component Analysis (PCA) and hierarchical clustered dendrogram on top of the heatmap of the extractable GCC abundances revealed four clades where MP2 and MP3 (Fig. 2A and B, turquoise and green); MP1 and MP12 (Fig. 2A and B, red and blue) formed single clades. The 95.7% of variance in PC1 in the PCA was primarily driven by differences in GCCs among the plots (Fig. 2B). The biplot analysis (Fig. 2C), indicated that P enrichment had the greatest impact on PC2, Cl on PC1, and K and Mg on both PC1 and PC2.

3.1.2. *Total GCCs*

The recovery rates from off-the-shelf GCCs estimated from aqua regia, analysed with ICP-AES exceeded 95 ± 1%. The identified total GCCs included Mg, K, Ca, Al, Mn, Fe, Cu, Na, As, Cd, Co, Cr, Mo, Ni, Pb, Ti, and Zn. Among these, Mg, Ca, Fe, Ni and Al exhibited statistically significant variability across plots ($p < 0.05$). Notably, K and Cr showed significance in MP6 and MP12 ($p < 0.05$); Na was low in MP1 as well as Co and Mo in MP12 (Table 1). Mn, Zn, Cd, As, Cu were constant across all plots, and Cu in MP12 compared to the other plots ($p < 0.05$). A visual heatmap representation of these findings are presented in Fig. 3A.

Ephaptic factors had limited influence, proton activity was positively correlated with K and Ca (R^2 = 0.51–0.69) while OC positively associated with K (R^2 = 0.88) and negatively with Al (R^2 = 0.54; Table S2). Inter GCCs correlation analysis revealed the following positive associations: Mn with Fe, Cu, As, Cd, and Co (R^2 = 0.51–0.97); Fe with Cu, As, and Cd (R^2 = 0.69–0.90); As with Cd (R^2 = 0.79); Cd with Co (R^2 = 0.51) and Ni with Zn (R^2 = 0.52; Table S2). Mixed correlation were observed. For instance, Co was positively corelated with Ni (R^2- 0.97) and negatively with Cr and Mo (R^2 = 0.86–0.87); Mg was positively corelated with Cu, Co, and Ni (R^2 = 0.56–0.95) and negatively with Cr and Mo (R^2 = 0.90–0.91); Al was corelated positively with Mn, Fe, Cu, As, Cd and Co (R^2 = 0.50–0.90) but negatively with Na (R^2 = 0.50); Cu was positively correlated with Cd, Co and Ni (R^2 = 0.51–0.90) but negatively with Na (R^2 = 0.54); Cr was positively and negatively corelated with Mo and Ni (R^2 = 0.99–0.99) respectively. Mo was negatively corelated with Ni (R^2 = 0.91; Table S2).

Hierarchical cluster in the PCA analysis revealed three clusters; MP1, MP3 MP5 (Fig. 3A and B, red, green, and yellow); MP2 and MP6 (Fig. 3A and B, light blue and magenta) and MP2 (Fig. 3A and B, blue). Over 61.3% of the variance was attributed to inter-plot element differences in GCC composition (Fig. 3B). The biplot analysis indicated that PC2 was influenced by Mg, Fe, Al, and Ni while Ti and Ca contributed to both components (Fig. 3C).

3.1.3. *Comparison of the extraction protocols for total and extractable GCCs*

In comparing common GCC abundances in aqua regia (AES) and Palin soil test kit (PT) extracts namely, K, Mg, Ca, Al, Mn, Fe, Cu), clear trends emerged. Aqua regia extracts consistently yield lower mean values for K (7.12 vs 143.82), Mg (39.7 vs 101.9), Cu values (1.59 vs 35.1), Ca (94.9 vs 2812.5) resulting in differences of −136.70, −62.22, −33.47, −2717.53 respectively. Mn showed a minor difference of −1.44, (aqua regia extract, 6.11; Palin soil test kit extract, 7.55). Conversely, Al and Fe displayed significant differences of 143.38 and 172.44, respectively, indicating higher values in the aqua regia extracts (155.99 and 229.49)

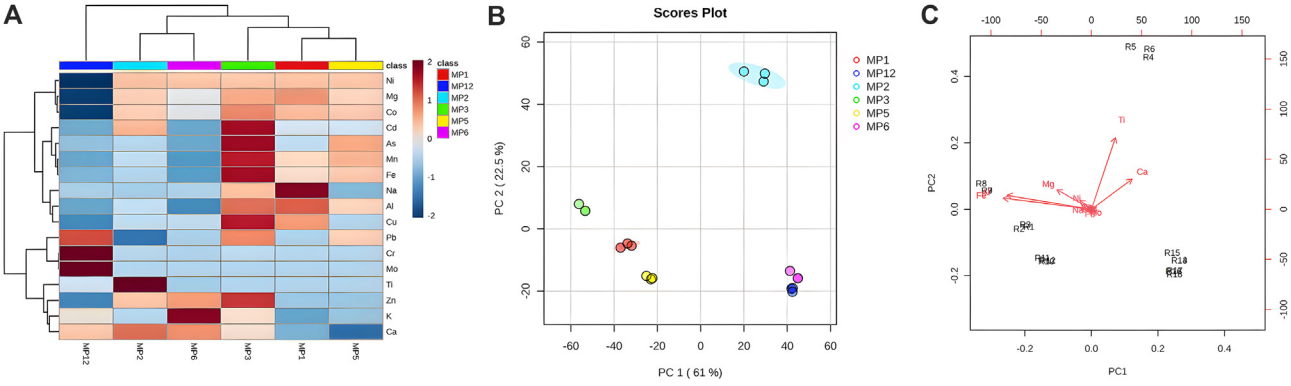

Fig. 3. Multivariate analysis of the GCCs content in 6 plots of an allotment from aqua regia extracts. Heatmap (A), PCA (B) and (C) biplot analysis of GCCs extracted from 1g of soil suspension using the aqua regia extraction protocol analysed with the Thermo Electron iCAP 6000 series ICP-AES. Key for replicates in each plot: MP1, R1-3; MP2, R4-6; MP3, R7-9; MP5, R10-12; MP6, R13-15; MP12, R16-18.

compared to Palin soil test kit extracts (12.61 and 57.05). Also, ranges for K (6.26 to 9.49), Mg (37.3 to 51.0), and Cu (1.38 to 2.28) in the aqua regia extracts were narrow compared to Palin soil test kit extract (88.3 to 285.0, 59.3 to 210.3, and 22.4 to 54.9, respectively). Strong relationships were obtained for K, Ca, and Cu (R^2 = 0.67–0.93) between these mean values from both extracts.

Heatmap analysis revealed Cu, K, Mg, Ca as the major sources of variation in the Palintest soil kit extracts while Al and Fe played this role for the aqua regia extracts (Fig. 4A). Hierarchical cluster dendrogram on the heatmap and PCA analysis revealed two distinct clusters for both extraction protocols and within each were two subclusters namely, MP6-AES, MP12-AES (Fig. 4A and B, blue, magenta) and MP1-AES, MP3-AES, MP2-AES, MP5-AES (Fig. 4A and B, green, red, light blue and yellow) for aqua regia. For the Palintest GCC extracts the sub clusters were composed of MP1-PT, MP5-PT (Fig. 4A and B, red, and yellow), and MP6-PT, MP12-PT, MP3-PT, MP3-PT (Fig. 4A and B, magenta, blue, light blue, and green).

3.2. Estimating the soil microbiome population and sensitivity to stressors

Acanthamoeba present in soil suspension were recovered as irregular patches on the surfaces of the nutrient deficient medium with recovery times varying in a density dependent manner (Fig. S1). For instant, colonies comprised of predominantly cysts appeared in medium containing MP6 and MP5 extracts at 5 and 14 days respectively (Table 2). These duration corelated well with the estimated *Acanthamoeba* biomass being $9.76 \pm 1.19 \times 10^9$ and $105 \pm 1.56 \times 10^9$ cells/ml respectively (Table 2). The *Acanthamoeba* species identified *Acanthamoeba* spp. are detailed in Table S4. A*canthamoeba* biomass showed strong positive correlations with OC, Mg, K, Fe, S and NH_4^+ (R^2 = 0.76–0.91).

To simplify the labour-intensive cell density estimations of *Acanthamoeba* via isolation with selective agar, we piloted a molecular approached for the quantification using Ct values obtained by qPCR with *Acanthamoeba* specific primers, against those in a standard curve produced with known *Acanthamoeba* cell density. The linear equation ($y = 2 \times 10^9 x - 6x10^7$, R^2 = 0.99; Fig. S2) applied to the Ct values, estimated *Acanthamoeba* densities to be 9.76×10^9 cells/mL and 105×10^9 *Acanthamoeb*a cells/mL for MP5 and MP6, respectively (Table 2). The correlation between the culture and molecular approach was R^2 = 0.59. Interestingly, associations identified previously between *Acanthamoeba* biomass and extractable GCCs were maintained namely with OC, Mg, K, S and NH_4^+ (R^2 = 0.57–0.79) but new associations emerged. For instance, positive association was observed between *Acanthamoeba* biomass and

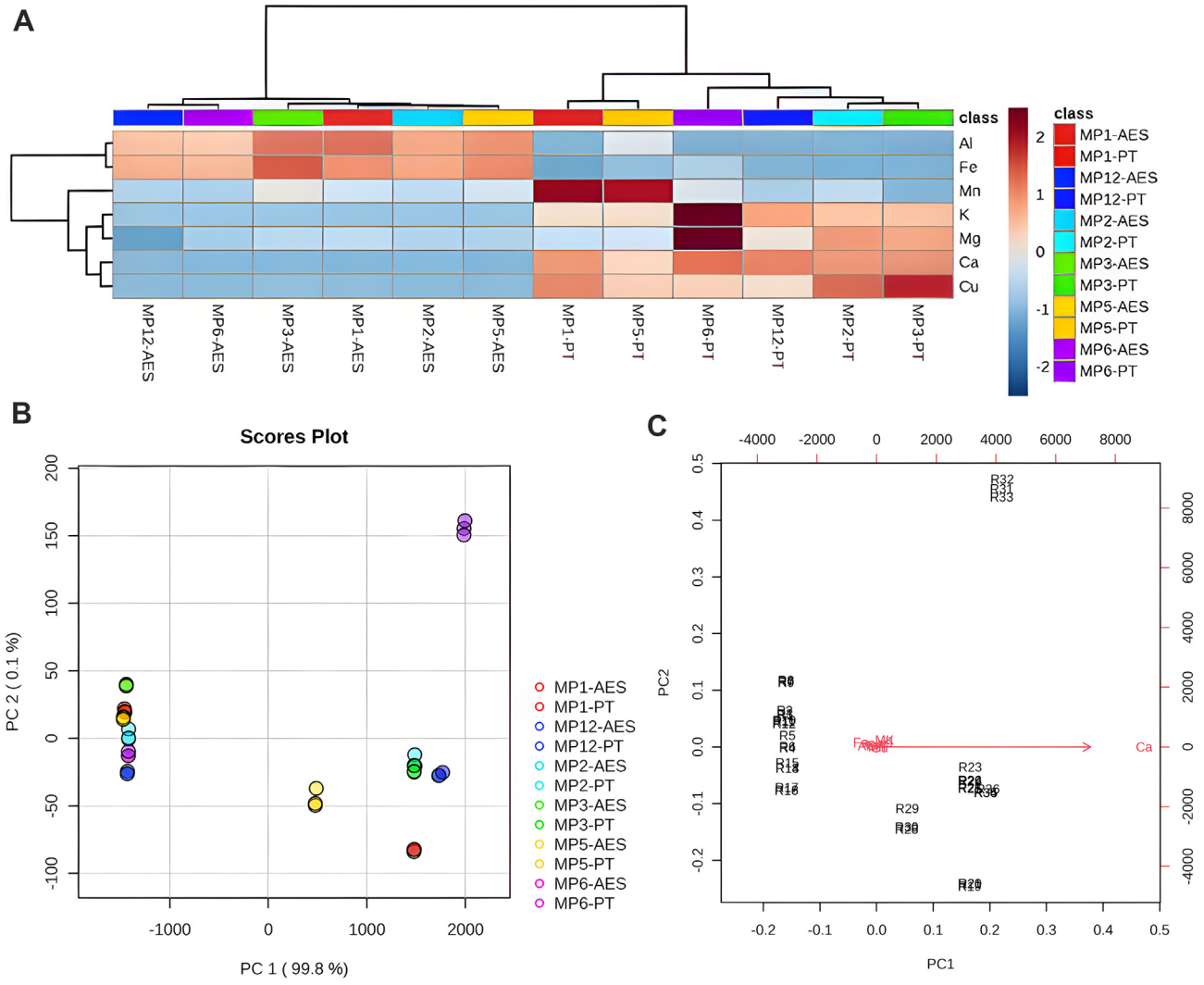

Fig. 4. Multivariate analysis of the GCCs content in 6 plots of an allotment using two analytical techniques. PCA (A), biplot (B) and heatmap (C) analysis of GCCs extracted using the Palintest soil (represented as MP1 – MP12-PT) and aqua regia extraction protocols (MP1-MP12-AES) on 1g of soil suspension. The GCC abundances were determined with the Soiltest 10 photometer and the Thermo Electron iCAP 6000 series ICP-AES respectively. Only GCCs common to both protocols were used in this analysis. Key for replicates in each plot: MP1, R1-3 (AES), R19-R21 (PT); MP2, R4-6 (AES), R2-R24 (PT); MP3, R7-9 (AES), R25-27 (PT); MP5, R10-12 (AES), R28-30 (PT); MP6, R13-15 (AES), R31-R33 (PT); MP12, R16-18 (AES), R34-36 (PT).

Table 2
Microbial biomass load and DNA content, and molecular estimation of *Acanthamoeba* biomass in 6 plots in an allotment.

Biological Indicators							
Prokaryotes biomass estimations	Temp, °C	MP1	MP2	MP3	MP5	MP6	MP12
Microbial load (cfu/g x 10^4)	25	1.04 ± 1.00	3.03 ± 1.00	1.25 ± 1.01	0.93 ± 1.02	4.25 ± 1.25	2.38 ± 1.34
	37	9.10 ± 1.22	2.03 ± 1.29	2.79 ± 1.12	1.30 ± 1.00	4.32 ± 1.23	2.55 ± 1.24
	55	4.20 ± 1.00	8.57 ± 1.33	1.29 ± 1.26	0.67 ± 1.65	6.62 ± 1.78	0.76 ± 0.94
Total no. of microbial load (cfu/g x 10^4)		14.43 ± 1.03	13.62 ± 1.25	5.33 ± 1.15	2.87 ± 1.35	15.20 ± 1.50	5.69 ± 1.25
Eukaryotes biomass estimation		MP1	MP2	MP3	MP5	MP6	MP12
Total *Acanthamoeba* load (x10^9 cells)		9.92 ± 1.23	9.80 ± 1.34	9.78 ± 1.56	9.76 ± 1.19	105.00 ± 1.56	9.98 ± 1.00
Colony appearance on non-nutrient agar plates duration		13.00 ± 2.00	12.00 ± 2.00	6.00 ± 2.00	14.00 ± 1.00	5.00 ± 1.00	7.00 ± 2.00
Molecular estimations		MP1	MP2	MP3	MP5	MP6	MP12
Total DNA content (µg/mL)		40.75 ± 2.98	39.1 ± 2.11	51.05 ± 3.45	28.6 ± 1.56	74.95 ± 3.87	59.5 ± 2.76

proton activity, Ca and CEC (R^2 = 0.72–0.89) and negatively with lime requirement (R^2-0.77). In the total extracts *Acanthamoeba* biomass was only positively associated with K derived from the cell culture method (R^2 = 0.82) and molecular approach (R^2 = 0.80). Notably we observed that *Acanthamoeba* thrived across a range of pH values, from acidic to alkaline, but was more abundant in plots with higher proton activity, particularly in MP6. The impact of pH on *Acanthamoeba* biomass was tested with the Alamar blue® cytotoxicity assay with estimated IC_{50}s of 0.0, 0.63 and 1.9 µg/mL at pH 3.6, 4.6 and 8.6 respectively, confirming pH-sensitivity. Association with bacteria at 25 °C and *Acanthamoeba* biomasses was also identified (R^2 = 0.6).

Bacteria biomasses were extracted from soil extracts at three temperatures. Assuming that each bacterial colonies obtained in the agar plates at these temperatures were unique, the total biomass for the 6 plots ranged from 2.87 × 10^4 (MP5) to 1.5 × 10^5 cfu/g (MP6, Table 2). Bacteria biomass at 25 °C for extractable GCCs displayed positive associations with OC, CEC, Mg, and K (R^2 = 0.59–0.76) from the extractable GCCs extracts. This same bacteria populations displayed associations positively with K, and Ca, (R^2 = 0.63–0.66 respectively) and negatively with Al, Mn, Fe, and As (R^2 = 0.50–0.70) in the total GCCs extracts. In these same extracts, bacteria isolated at 37 °C were associated negatively with Na (R^2 = 0.80) and at 55 °C with negatively with Pb (R^2 = 0.73) and positively with CEC (R^2 = 0.54).

MP5 with the lowest microbial load (2.87 × 10^4 ± 1.35 cfu/g) showed high Al, and the impact of this PTE was assessed. Bacteria colonies were isolated only from MP5 soil suspensions on nutrient agar plates containing 10 mM Al, after 72 h, confirming the impact of Al on bacteria biomass. Molecular identification of the bacteria isolated using differences in the 16srRNA gene sequences revealed *Bacillus* spp. strains, *Burkholderia* spp., and *Micrococcus* spp. (Table S3).

3.3. Soil quality index estimations

The Soil Quality Index (SQI) was determined using a set of extractable GCCs, which are considered reliable indicators for estimating soil quality. These indicators encompassed various factors, including edaphic factors (proton activity, OC, EC, CEC), nutrient concentrations (such as N, P, and K), specific elements (e.g., Ca, Mg, and Fe), and microbial populations (prokaryotic and eukaryotic biomasses).

Each of these indicators was categorized into distinct ranges, and for each range, an interpretation was provided regarding its impact on soil quality (Table S5). These interpretations were based on established criteria previously published (O'Neill et al., 2005; Mukherjee and Lal, 2014). To assign scores, for the purpose of calculating the SQI, a numerical scale ranging typically from 0 to 3 was used. A score of 0 indicated a negative to low impact, while 3 signified the highest positive impact on soil quality.

To compute the SQI for each plot, these scores were applied to the measured values in that plot. The sum of scores across all indicators for each plot was then expressed as a percentage of the total achievable score, resulting in the overall SQI value for that plot. In our study, the calculated SQI, for the different plots ranged from 23 to 37, corresponding to percentages of the total available score ranging from 42.5 to 68.5%. Notably, MP6 exhibited the highest SQI, indicating healthier soil quality, while MP5 had the lowest SQI, signifying relatively poorer soil quality (Table S5). These SQI values were positively corelated with pH, Ca, S, CEC (R^2 = 0.50–0.94) and negatively with EC, lime requirement, Al, P and *Acanthamoeba* biomass derived with the molecular approach (R^2 = 0.62–0.88).

3.4. Acanthamoeba has a functional assimilatory/dissimilatory nitrate reduction pathway for N- recycling

The varied NO_3-:NH_4^+ratio of 5.3–0.69 in MP5/6 indicated a high turnover prompted us to investigate the role of *Acanthamoeba* in this process using a combination of approaches (Table 1). Initial *in-silico* analysis of the *Acanthamoeba* gene content did not identify a gene with significant identity with known NO_3^- transporter. Nevertheless, the reduction of nitrate was observed in complete PG medium containing 6.94 mg/L NO_3^-, with an inoculum of 10^5 *Acanthamoeba* after 5 days by 44% ([NO_3^-] to 3.89 mg/L (Fig. 5) a mechanism of nitrate uptake via an as-yet-unknown transporter.

Concurrently there was an increase in [NH_4^+] from 0.003 to 0.04 mg/mL, suggesting its release into the media from an intracellular assimilation pathway for NO_3^- to NH_4^+ conversion (Fig. 5). Further, in silico analysis revealed the presence of six NH_4^+ transporters in *Acanthamoeba* belonging to three families. These included the structurally related membrane transport proteins (AMT, ACA1_230500; Fig. S7, top clade), methylammonium/ammonium permeases (MEP; ACA1_362530, ACA1_362520; Fig. S7, middle clade) and Rhesus (Rh; ACA1_138770, ACA1_065130, ACA1_098420; Fig. S7, bottom clade). Intracellular levels of [NO_3^-], to [NO_2^-] and [NH_4^+] were 0.28 mg/L, 0.029 mg/L and 1.32 mg/L respectively (Fig. 5).

Further, we identified translated amino acids of AcNR, (927 residues, ACA1_054310) and comparison with characterise orthologues allowed us to identify its two-domains held together by a hinge region, each with binding motifs for molybdopterin, cytochrome *b*5, NAD, and FAD (Fig. S3). The enzymatic activity of AcNR was 0.79 units/mg/min in *Acanthamoeba* lysates (0.5 mg/mL), suggesting the capacity of the protist to undertake [NO_3^-] to [NO_2^-] conversion (Fig. 5). Translated amino acids sequences of AcNIR (186 residues, ACA1_134610), with one (Fig. S4) as opposed to the two motifs cupredoxin motif reported for all known orthologues was identified in *Acanthamoeba* gene content, suggesting the capacity of the protist to undertake to [NO_2^-] to [NH_4^+] conversion and a complete assimilatory/dissimilatory nitrate reduction pathway in the protist (Fig. 5A).

4. Discussions

The use of two extraction protocols namely the aqua regia and Palin soil test kit, combined with comprehensive multivariate and correlation

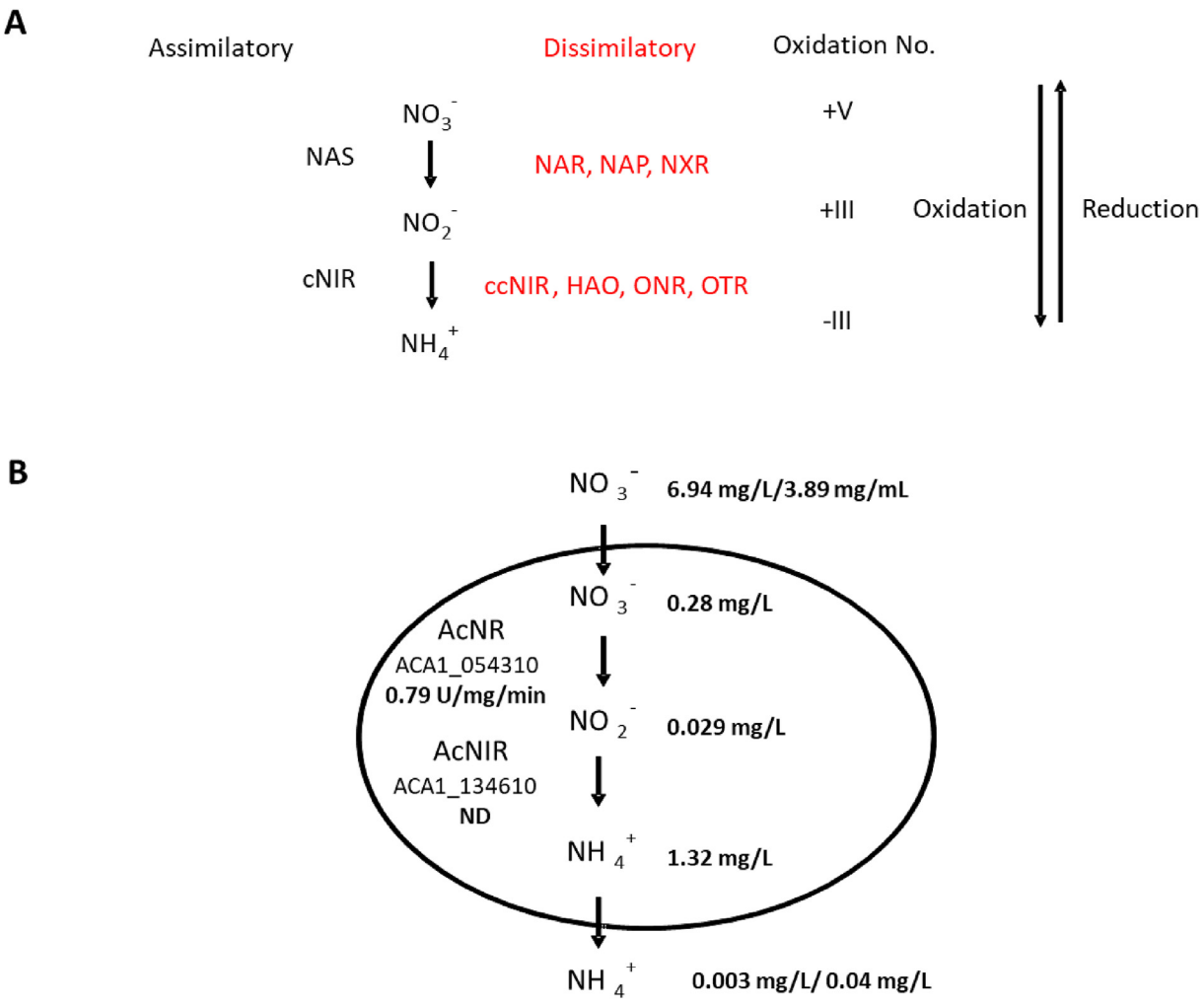

Fig. 5. Nitrogen transformations in *Acanthamoeba*. (A) The oxidative reaction of the nitrogen assimilatory pathway (black) showing the conversion of nitrates (NO_3^-) to ammonium (NH_4^+) via nitrites (NO_2^-) and associated enzymes nitrate reductase (NAS) and nitrite reductase (cNIR). The reverse reductive process, the nitrogen dissimilatory pathway (red) utilizes the enzymes NAR, NAP, NXR and ccNIR, HAO, ONR, OTR respectively. The varied oxidation numbers of N during these conversions are presented. (B) A single *Acanthamoeba* cell depicted as a circle represents 10^5 cells/mL *Acanthamoeba* in PG medium that contained 6.94 mg/L nitrate (NO_3^-) and 0.003 mg/L ammonium (NH_4^+). After incubation for up to 5 days in in vitro culture, the NO_3^- and NH_4^+ measured form spent medium were 3.98 mg/mg/L and 0.04 mg/L respectively. Within the *Acanthamoeba* cell, intracellular NO_3^-, NO_2^-, and NH_4^+ concentrations estimates were 0.28 mg/L, 0.029 mg/L and 1.32 mg/L respectively. The enzymatic activity of nitrate reductase (AcNR) in *Acanthamoeba* lysate (0.05 mg) was determined to be 0.79 U/mg/min. NO_3^-, NO_2^-, and NH_4^+ were determined by the nitrite/nitrate (Sigma Aldrich, UK), and Ammonium (Sigma Aldrich, UK) assay kits. **Key**: NAS, assimilatory nitrate reductase; NAP, periplasmic nitrate reductase; NXR, Nitrate-oxidoreductase; NAR, respiratory nitrate reductase; cNIR, nitrite reductase; ccNIR, cytochrome *c* nitrite reductase; ONR, octahemic nitrite reductase; OTR, octaheme tetrathionate reductase; HAO, octahaem hydroxylamine oxidoreductase.

analysis at the Wellington Allotment, has enabled us to differentiate the disparities between extractable and total GCCs content. This investigation has also shed light on the intricate interactions between these enriched GCCs and microbiota, with a unique focus on the role of the eukaryotic organism, *Acanthamoeba* (Table 1). Our initial insight was drawn from mean differences of GCC estimations, notably, the aqua regia extracts exhibited higher estimates for Al and Fe, while the Palin soil test kit extracts yielded lower estimates for K, Mg, Cu, and Ca. Furthermore, the Palin soil test kit extracts exhibited wider ranges. This observation can be attributed to differences in the extraction protocols, elemental specificity, inherent characteristics of the aqua regia method, and sensitivities or detection limits for specific elements across analytical techniques underscoring the distinction between extractable and total GCCs.

4.1. *Significant interconnections were observed among edaphic parameters*

Significant interconnections were observed among edaphic parameters, including pH, OC, EC, and CEC, particularly within the Palin soil test kit extracts, although they were less pronounced in aqua regia extracts. For instance, in the Palin soil test kit extracts, proton activity correlated positively with Mg, Ca, and S, and negatively with Al, Mn, and P (Tables 1 and S1). In contrast, in the aqua regia extracts, positive correlation was limited to K and Ca (Tables 1 and S2). These observations are influenced by the choice of extraction protocols (Al-Soghir et al., 2022; Hammam et al., 2022). Soil properties such as CEC and OC, which are also impacted by proton activity-GCC interactions, exhibited significant correlations mirroring proton activity. In contrast, EC exhibited a reverse trend for the same subset of GCCs, suggesting that the Palin soil test kit extract more accurately replicates the natural soil environment.

Inter-GCC correlations among the extractable GCCs, such as S and NH_4^+ or K with Fe, S, and NH_4^+, as well as Fe with S and NH_4^+, and Mg with K, Fe, S, and NH_4^+, provide deeper insights into how these GCCs interact. This reveals possible mutual, synergistic, or antagonistic relationships that may impact their availability. For example, the negative association of P with Cl, Ca, and the positive association with Al and Mn may provide insights into how these GCCs influence P availability

(Tables 1 and S1) (Nieder et al., 2018). These quantitative correlations complement the results obtained from multivariate statistics, such as Principal Component Analysis (PCA), which helped reduce the dimensionality of our complex datasets. This not only enhances our overall understanding but also boosts our confidence in the results.

Total extracts obtained through the aqua regia extraction method revealed interactions among PTEs, indicating co-occurrence and similar geological processes (Nieder et al., 2018). For instance, Cu, Co, Cr, Mo, Ni, and Zn showed significant interactions, while Fe, Mn, As, and Cd reflect the prevailing redox state of the soil (Tables 1 and S2) (Nieder et al., 2018). The documented history of the Wellington allotment with respect to PTEs, such as Cu, Cd, As, and Ni from anthropogenic sources associated with various industrial processes, may explain the presence of these contaminants. Similarly, the interaction of pH with K and Ca may be linked to their influence on the buffering and ion exchange capacity of soils, while the association of OC with K and Al may be influenced by environmental and geochemical factors.

4.2. Soil chemistry influenced soil microbiota

We have also explored the influence of soil chemistry on soil microbiota, focusing on the total bacterial population isolated at different temperatures (25 °C, 37 °C, and 55 °C) and *Acanthamoeba* as representatives of prokaryotes and eukaryotes, respectively.

The *Acanthamoeba* biomass retrieved from all plots exhibited positive correlations with various factors. These included OC, Mg, K, Fe, S, and NH_4^+, which aligned with nutrient availability in the Palin soil test kit extract. In contrast, *Acanthamoeba* biomass correlated positively with K alone in the aqua regia extract underscoring the significance of K as an essential nutrient for *Acanthamoeba* biomass, along with OC, Mg, Fe, S, and NH_4^+ (Hashim et al., 2015). Notably, these correlations were only evident when using the Palin soil test kit, reinforcing its utility for providing biologically relevant data on soil biochemistry using a cost-effective and field-accessible kit.

Furthermore, we explored an alternative species-specific molecular approach for estimating *Acanthamoeba* biomass. This method leveraged Ct values obtained through qPCR amplification of 18srRNA using total soil DNA as a template. Remarkably, this molecular approach demonstrated a significant correlation with our traditional method, and OC, Mg, K, Fe, S, and NH_4^+. Moreover, the molecular approach revealed novel correlations with pH, CEC, Ca, and lime requirements, which have biological relevance. Notably, *Acanthamoeba* exhibited pH-dependent behaviour in cytotoxicity assays at pH 3.6, 4.6 and 8.6, and its interaction with lime and Ca may serve to mitigate pH and metal toxicity (Bide et al., 2021). The application of this molecular approach has become feasible with compact, ruggedized, battery-powered handheld or portable qPCR devices like the Biomeme Franklin Real-Time PCR Thermocycler, making it adaptable outside traditional laboratory settings. Extending this approach to include prokaryotes, including their unculturable counterparts (Amann et al., 1990), and other eukaryotes is now plausible. Furthermore, the collection of total DNA from environmental materials, such as soils, is supported by extraction kits (Zymo Research (ZR) Soil Microbe DNA MiniPrep kit (Catalog No. D6001). This approach has seen extensive use in environmental DNA (eDNA) research across aquatic (Nevers et al., 2018) and soil environments (Wutkowska et al., 2018), where DNA isolation can be challenging but has been conducted successfully with high accuracy.

4.3. Acanthamoeba and bacteria played roles in NO_3^-/NH_4^+ recycling and microbial ecology

A notable observation concerning *Acanthamoeba* was its potential role in NO_3^-/NH_4^+ recycling (Yao et al., 2013; Maeda et al., 2011; Einsle et al. 1999, 2000). In silico analysis revealed that *Acanthamoeba* possesses translated amino acid sequences for genes encoding three families of NH_4^+ transporters: AMT, Rh, and MEP, facilitating NH_4^+ uptake and release. Additionally, genes encoding nitrate reductase and nitrite reductase (designated AcNR and AcNIR) from the assimilatory/dissimilatory nitrate reduction pathway were identified, enabling the enzymatic reduction of NO_3^- to NO_2^- and subsequently NH_4^+ (Burger and Jackson, 2004). Notably, no gene encoding NO_3^- transporter genes displayed significant homology with orthologs from other taxa in our BLAST search (Figs. S3–S7). The functionality of this pathway in this protist was confirmed by a 44% decrease in NO_3^- and a 1233% increase in NH_4^+ in the external milieu of *Acanthamoeba* in vitro cultures, the presence of intermediates of assimilatory/dissimilatory nitrate reduction, and enzymatic activity of AcNR in *Acanthamoeba* lysates (Fig. 5). This reduction of NO_3^- and concurrent increase in NH_4^+ suggests the presence of a species-specific transporter and release of NH_4^+ into the external environment to modulate soil NH_4^+ levels respectively (McDonald and Ward, 2016). This replenishment of NH_4^+ in the soil is particularly relevant for plants like Chinese cabbage, lettuce, and spinach cultivated in this plot, known for their high NH_4^+ requirements (Song et al., 2012). These findings underscore the complexity of nitrogen cycling in soil ecosystems, previously attributed primarily to prokaryotic soil microbiota, which also involves eukaryotic soil biota (McCarty and Bremner, 1992; Burger and Jackson, 2005).

Bacteria biomass isolated at 25 °C had significant correlations with key soil properties, such as CEC, OC, Mg, Ca, and K within the extractables. These findings underscore the crucial role of cation retention and nutrient regulation in microbial ecology (Coonan et al., 2020). Conversely, we noted negative correlations between bacterial biomass and PTEs like Al, Mn, Fe, and As. These negative correlations coincided with PTE known to suppressed microbial communities (Coonan et al., 2020).

While our study did not reveal direct correlations between pH and bacterial biomass, we did find an intriguing pattern in one location, MP5. Here, a low pH was associated with reduced microbial biomass and elevated levels of Al (Tables 1 and 2). Surprisingly, this specific location harboured microbial species like *Bacillus* spp., *Burkholderia* spp., and *Micrococcus* spp., which exhibited remarkable adaptation to Al as high as 10 mM (Table S3). This phenomenon highlights the bioremediation potential of the microbiota at this site (Salem et al., 2012). Effective management strategies, such as lime application (Álvarez et al., 2005; Bide et al., 2021), are essential to counteract Al toxicity and pH imbalances. Ongoing monitoring is critical for developing timely remediation strategies and preventing long-term adverse effects of PTEs at this site.

The significant correlation observed between *Acanthamoeba,* and bacterial biomasses aligns with documented symbiotic and trophic relationships reported between these two taxa, including interactions with *Legionella pneumophila*, *Mycobacterium avium*, *Bacillus* spp., *Escherichia coli, Chlamydia trachomatis*, and *Burkholderia* spp. (Rayamajhee et al., 2021). These intricate relationships, combined with the specific requirements of microorganisms and their interactions with GCCs and metabolic pathways, have motivated us to develop a Soil Quality Index (SQI) to safeguard soil health.

4.4. Functional-based SQI was influenced by several key parameters

Our soil quality index (SQI) draws inspiration from the work of (O'Neill et al., 2005; Mukherjee and Lal, 2014), which integrated at least nine soil quality indicators that revolved around soil functional attributes related to root development and nutrient storage, identified through a literature review, supplemented with subjective scoring. In our approach, we have adopted a similar framework, focusing on soil functional attributes related to microbial biomass and have added a biological addendum, to make our SQI more function based.

The resulting SQI was influenced by several key parameters including pH, S, Ca, CEC, and *Acanthamoeba* biomass. The estimation of *Acanthamoeba* biomass utilizes molecular techniques that encompass biomass production. Interestingly, our SQI exhibits negative correlations with factors like EC, lime requirements, Al, and P, which mirror the negative determinants of biomass production, further underscoring the SQI's

effectiveness in predicting soil quality. It is essential to recognise that a broader array of parameters has contributed to enhancing the validity of our estimated SQI while a comparative analysis of three SQI approaches (O'Neill et al., 2005; Mukherjee and Lal, 2014) indicated that a lower number of selected indicators exhibited relatively higher correlations with crop yield, making it the most promising method. Nevertheless, our study and the inclusion of additional chemical and biological parameters have contributed to strengthening the validity of SQIs using our approach.

In our comparison between a soil function-based approach and the principal component analysis (PCA) approach, the soil function-based method emerged as superior methodology (Lenka et al., 2022). Similarly, when comparing four quantitative approaches namely the PCA, PCA-percentile, soil function-based and the soil function-based-percentile methods, it became evident that the soil function-based approach outperformed PCA in terms of achieving higher correlations between SQI and rice and wheat yields. Notably, the percentile method displayed stronger correlations in both PCA and soil function-based methods (Lenka et al., 2022). Consequently, it was shown that the soil function-based approach, combined with the percentile method for data transformation, proved to be the superior method for computing SQI and establishing a relationship with production function.

5. Conclusions

In summary, our study has explored the intricate relationship between soil chemistry and microbial communities, particularly *Acanthamoeba*, highlighting their pivotal role in sustaining nitrogen recycling processes within soils but has underscored the urgent need for proactive measures to control and prevent soil pollution. Overall, our study provides a good understanding of microbiota interactions in soil, and the development of an effective SQI for soil quality assessment. The SQI developed can serve as a good monitoring tool based on fundamental soil characteristics that facilitates the assessment of soil health and improvement, and empower land users with the means to directly evaluate soil health over time, which aligns with the broader objectives of the One Health approach, emphasizing the intricate interconnections between soil fauna, soil chemistry, and human activities. Consequently, our study highlights the critical role of soil health in the larger context of environmental well-being, serving as a call to action for more comprehensive soil management practices and continued research in this field to address the challenges posed by soil pollution and ensure a sustainable soil resource. Future study should employ a large database to verify our conclusion and improve the soil quality index.

Declaration of Competing Interest

The authors declare that they have no known competing financial interests or personal relationships that could have appeared to influence the work reported in this paper.

Acknowledgements

This study has been funded by the IBEHR ECR fund, and PhD programme of School of Andrea Ogoke, School of Health and Life Science, University of the West of Scotland.

Appendix A. Supplementary data

Supplementary data to this article can be found online at https://doi.org/10.1016/j.seh.2023.100046.

References

Al-Soghir, Mostafa, M.A., Mohamed, Ahmed G., El-Desoky, Mohamed A., Awad, Ahmed A.M., 2022. Comprehensive assessment of soil chemical properties for land reclamation purposes in the toshka area, Egypt. Sustainability 14, 15611.

Alloway, B.J., Charles Ayres, David, 1993. Chemical Principles of Environmental Pollution (Blackie Academic & Professional: London London, New York, Blackie Academic & Professional, 1993.).

Álvarez, E., Fernández-Marcos, M.L., Monterroso, C., Fernández-Sanjurjo, M.J., 2005. Application of aluminium toxicity indices to soils under various forest species. For. Ecol. Manag. 211, 227–239.

Amann, Rudolf I., Brian, J Binder, Robert, J Olson, Sallie, W Chisholm, Devereux, Richard, DA184531 Stahl, 1990. Combination of 16S rRNA-targeted oligonucleotide probes with flow cytometry for analyzing mixed microbial populations. Appl. Environ. Microbiol. 56, 1919–1925.

Balaram, V., 2021. Strategies to overcome interferences in elemental and isotopic geochemical analysis by quadrupole inductively coupled plasma mass spectrometry: a critical evaluation of the recent developments. Rapid Commun. Mass Spectrom. 35, e9065.

Bargaz, A., Lyamlouli, K., Chtouki, M., Zeroual, Y., Dhiba, D., 2018. Soil microbial resources for improving fertilizers efficiency in an integrated plant nutrient management system. Front. Microbiol. 9.

Bastida, F., Eldridge, D.J., Garcia, C., Kenny Png, G., Bardgett, R.D., Delgado-Baquerizo, M., 2021. Soil microbial diversity-biomass relationships are driven by soil carbon content across global biomes. ISME J. 15, 2081–2091.

Bechet, B., Joimel, S., Jean-Soro, L., Hursthouse, A., Agboola, A., Leitao, T.E., Costa, H., Cameira, M.D., Le Guern, C., Schwartz, C., Lebeau, T., 2018. Spatial variability of trace elements in allotment gardens of four European cities: assessments at city, garden, and plot scale. J. Soils Sediments 18, 391–406.

Ben-David, A., Davidson, C.E., 2014. Estimation method for serial dilution experiments. J. Microbiol. Methods 107, 214–221.

Bide, T., Ander, E.L., Broadley, M.R., 2021. A spatial analysis of lime resources and their potential for improving soil magnesium concentrations and pH in grassland areas of England and Wales. Sci. Rep. 11, 20420.

Burger, M., Jackson, L.E., 2004. Plant and microbial nitrogen use and turnover: rapid conversion of nitrate to ammonium in soil with roots. Plant Soil 266, 289–301.

Burger, M., Jackson, L.E., 2005. Plant and microbial nitrogen use and turnover: rapid conversion of nitrate to ammonium in soil with roots. Plant Soil 266, 289–301.

Coonan, Elizabeth C., Kirkby, Clive A., Kirkegaard, John A., Amidy, Martin R., Strong, Craig L., Richardson, Alan E., 2020. Microorganisms and nutrient stoichiometry as mediators of soil organic matter dynamics. Nutrient Cycl. Agroecosyst. 117, 273–298.

Einsle, O., Messerschmidt, A., Stach, P., Bourenkov, G.P., Bartunik, H.D., Huber, R., Kroneck, P.M.H., 1999. Structure of cytochrome c nitrite reductase. Nature 400, 476–480.

Einsle, O., Stach, P., Messerschmidt, A., Simon, J., Kroger, A., Huber, R., Kroneck, P.M.H., 2000. Cytochrome c nitrite reductase from Wolinella succinogenes - structure at 1.6 angstrom resolution, inhibitor binding, and heme-packing motifs. J. Biol. Chem. 275, 39608–39616.

Ertabaklar, H., Turk, M., Dayanir, V., Ertug, S., Walochnik, J., 2007. Acanthamoeba keratitis due to Acanthamoeba genotype T4 in a non-contact-lens wearer in Turkey. Parasitol. Res. 100, 241–246.

Gonzalez-Quinones, V., Stockdale, E.A., Banning, N.C., Hoyle, F.C., Sawada, Y., Wherrett, A.D., Jones, D.L., Murphy, D.V., 2011. Soil microbial biomass-Interpretation and consideration for soil monitoring. Soil Res. 49, 287–304.

Hammam, Amr A., Mohamed, Wagih S., Sayed, Safa Essam-Eldeen, Kucher, Dmitry E., Mohamed, Elsayed Said, 2022. Assessment of soil contamination using gis and multivariate analysis: a case study in el-minia governorate, Egypt. Agronomy 12, 1197.

Hashim, Fatimah, Rahman, Nur Athirah Abdul, Amin, Nakisah Mat, 2015. Morphological analysis on the toxic effect of manganese on Acanthamoeba sp. isolated from setiu wetland, terengganu: an in vitro study. Proced. Environ. Sci. 30, 15–20.

Hoogsteen, M.J.J., Lantinga, E.A., Bakker, E.J., Groot, J.C.J., Tittonell, P.A., 2015. Estimating soil organic carbon through loss on ignition: effects of ignition conditions and structural water loss. Eur. J. Soil Sci. 66, 320–328.

Huber, Sigbert, Syed, Bronwyn, Freudenschuss, A., Ernstsen, Vibeke, Peter, Loveland, 2001. *Proposal For a European Soil Monitoring and Assessment Framework* (EEA).

Idowu, O.J., van Es, H.M., Abawi, G.S., Wolfe, D.W., Schindelbeck, R.R., Moebius-Clune, B.N., Gugino, B.K., 2009. Use of an integrative soil health test for evaluation of soil management impacts. Renew. Agric. Food Syst. 24, 214–224.

Khan, N.A., 2006. Acanthamoeba: biology and increasing importance in human health. FEMS Microbiol. Rev. 30, 564–595.

Kumar, S., Nei, M., Dudley, J., Tamura, K., 2008. MEGA: a biologist-centric software for evolutionary analysis of DNA and protein sequences. Briefings Bioinf. 9, 299–306.

Lehmann, J., Bossio, D.A., Kogel-Knabner, I., Rillig, M.C., 2020. The concept and future prospects of soil health. Nat. Rev. Earth Environ. 1, 544–553.

Lenka, Kumar, Narendra, Prakash Meena, Bharat, Lal, Rattan, Khandagle, Abhishek, Lenka, Sangeeta, Shirale, Abhay Omprakash, 2022. Comparing four indexing approaches to define soil quality in an intensively cropped region of northern India. Front. Environ. Sci. 10.

Lilburne, L., Sparling, G., Schipper, L., 2004. Soil quality monitoring in New Zealand: development of an interpretative framework. Agric. Ecosyst. Environ. 104, 535–544.

Liu, P., Zhang, Y., Feng, N., Zhu, M., Tian, J., 2020. Potentially toxic element (PTE) levels in maize, soil, and irrigation water and health risks through maize consumption in northern Ningxia, China. BMC Publ. Health 20, 1729.

Maeda, K., Hanajima, D., Toyoda, S., Yoshida, N., Morioka, R., Osada, T., 2011. Microbiology of nitrogen cycle in animal manure compost. Microb. Biotechnol. 4, 700–709.

McBride, J., Ingram, P.R., Henriquez, F.L., Roberts, C.W., 2005. Development of colorimetric microtiter plate assay for assessment of antimicrobials against Acanthamoeba. J. Clin. Microbiol. 43, 629–634.

McCarty, Gregory W., Bremner, John M., 1992. Inhibition of assimilatory nitrate reductase activity in soil by glutamine and ammonium analogs. Proc. Natl. Acad. Sci. U.S.A. 89, 5834–5836.

McDonald, T.R., Ward, J.M., 2016. Evolution of electrogenic ammonium transporters (AMTs). Front. Plant Sci. 7, 352.
Moran, E.F., Packer, A., Brondizio, E., Tucker, J., 1996. Restoration of vegetation cover in the eastern Amazon. Ecol. Econ. 18, 41–54.
Mukherjee, A., Lal, R., 2014. Comparison of soil quality index using three methods. PLoS One 9.
Nelson, M.B., Martiny, A.C., Martiny, J.B., 2016. Global biogeography of microbial nitrogen-cycling traits in soil. Proc. Natl. Acad. Sci. U. S. A. 113, 8033–8040.
Nevers, M.B., Byappanahalli, M.N., Morris, C.C., Shively, D., Przybyla-Kelly, K., Spoljaric, A.M., Dickey, J., Roseman, E.F., 2018. Environmental DNA (eDNA): a tool for quantifying the abundant but elusive round goby (Neogobius melanostomus). PLoS One 13, e0191720.
Nieder, Rolf, Benbi, Dinesh K., Reichl, Franz X., 2018. Role of potentially toxic elements in soils. In: Nieder, Rolf, Benbi, Dinesh K., Reichl, Franz X. (Eds.), Soil Components and Human Health. Springer Netherlands, Dordrecht.
O'Neill, K.P., Amacher, M.C., Palmer, C.J., 2005. Developing a national indicator of soil quality on U.S forestlands: methods and initial results. Environ. Monit. Assess. 107, 59–80.
Pintro, J., Barloy, J., Fallavier, P., 1996. Aluminum effects on the growth and mineral composition of corn plants cultivated in nutrient solution at low aluminum activity. J. Plant Nutr. 19, 729–741.
Rayamajhee, B., Subedi, D., Peguda, H.K., Willcox, M.D., Henriquez, F.L., Carnt, N., 2021. A systematic review of intracellular microorganisms within Acanthamoeba to understand potential impact for infection. Pathogens 10.
Salem, Issam Ben, Sghaier, Haïtham, Trifi, Houda, Héni, Sana, Khwaldia, Khaoula, Saidi, Mouldi, Ahmed, Landoulsi, 2012. Isolation and characterization of a novel Micrococcus strain for bioremediation of strontium in radioactive residues. Afr. J. Microbiol. Res. 6.
Schoenholtz, S.H., Van Miegroet, H., Burger, J.A., 2000. A review of chemical and physical properties as indicators of forest soil quality: challenges and opportunities. For. Ecol. Manag. 138, 335–356.
Scotland. Communities Analytical Services, 2018. Scottish Vacant and Derelict Land Survey.
Sinclair, J.L., McClellan, J.F., Coleman, D.C., 1981. Nitrogen mineralization by Acanthamoeba polyphaga in grazed Pseudomonas paucimobilis populations. Appl. Environ. Microbiol. 42, 667–671.
Song, Shiwei, Yi, Lingyan, Liu, Houcheng, Sun, Guangwen, Chen, Riyuan, 2012. Effect of ammonium and nitrate ratios on growth and yield of flowering Chinese cabbage. In: Jin, David, Lin, Sally (Eds.), Advances in Multimedia, Software Engineering and Computing, vol. 1. Springer Berlin Heidelberg, Berlin, Heidelberg, pp. 227–232.
Teng, Yanguo, Wu, Jin, Lu, Sijin, Wang, Yeyao, Jiao, Xudong, Song, Liuting, 2014. Soil and soil environmental quality monitoring in China: a review. Environ. Int. 69, 177–199.
Trivedi, P., Delgado-Baquerizo, M., Trivedi, C., Hamonts, K., Anderson, I.C., Singh, B.K., 2017. Keystone microbial taxa regulate the invasion of a fungal pathogen in agro-ecosystems. Soil Biol. Biochem. 111, 10–14.
Williams, R.A.M., Smith, T.K., Cull, B., Mottram, J.C., Coombs, G.H., 2012. ATG5 is essential for ATG8-dependent autophagy and mitochondrial homeostasis in leishmania major. PLoS Pathog. 8.
Wu, S.C., Cao, Z.H., Li, Z.G., Cheung, K.C., Wong, M.H., 2005. Effects of biofertilizer containing N-fixer, P and K solubilizers and AM fungi on maize growth: a greenhouse trial. Geoderma 125, 155–166.
Wutkowska, M., Vader, A., Mundra, S., Cooper, E.J., Eidesen, P.B., 2018. Dead or alive; or does it really matter? Level of congruency between trophic modes in total and active fungal communities in high arctic soil. Front. Microbiol. 9, 3243.
Xia, J., Psychogios, N., Young, N., Wishart, D.S., 2009. MetaboAnalyst: a web server for metabolomic data analysis and interpretation. Nucleic Acids Res. 37, W652–W660.
Yao, H.Y., Campbell, C.D., Chapman, S.J., Freitag, T.E., Nicol, G.W., Singh, B.K., 2013. Multi-factorial drivers of ammonia oxidizer communities: evidence from a national soil survey. Environ. Microbiol. 15, 2545–2556.
Ylagan, S., Amorim, H.C.S., Ashworth, A.J., Sauer, T., Wienhold, B.J., Owens, P.R., Zinn, Y.L., Brye, K.R., 2021. 'Soil Quality Assessment of an Agroforestry System Following Long-Term Management in the Ozark Highlands, vol. 4. Agrosystems Geosciences & Environment.